



# Effects of Step Transverse Slopes on Locations of Inception Point of Flow over Stepped Spillways

Ahang S. Ali<sup>1</sup>, Omed S. Q. Yousif<sup>2\*</sup>

<sup>1</sup>University of Sulaimani, Sulaimani, Iraq, [ahang.ali@univsul.edu.iq](mailto:ahang.ali@univsul.edu.iq)

<sup>2</sup>University of Sulaimani, Sulaimani, Iraq, [omed.qadir@univsul.edu.iq](mailto:omed.qadir@univsul.edu.iq)

\*Corresponding author: Omed S. Q. Yousif, [omed.qadir@univsul.edu.iq](mailto:omed.qadir@univsul.edu.iq)

Published online: 30 September 2020

**Abstract**—In this experimental study, the effects of the steps having transverse slope in a zigzag pattern on the inception point location for flows over the stepped flat spillways were experimentally explored. Accordingly, three wooden stepped spillways were erected in a rectangular flume and tested under several discharges; ranging from 0.003 to 0.05 m<sup>3</sup>/s. The dimensions of the stepped spillways, each has thirty-two steps, were 0.605 m, 0.96 m, and 1.92 m for the width, depth, and length respectively. Thirty-two steps (with three different transverse slopes ranging from zero to 2.84°) were cut into the surface of the models from the crest to the toe. From the results, it was found that the distances of the inception points from the downstream edge of the spillway crest were decreased by 37%, on average, for the stepped spillways with steps having a transverse slope of 2.84°. It was also found that the onset of the skimming flow for the stepped spillways with steps having the transverse slope occurred at higher discharges;  $y_c/h \geq 2.06$ . In addition, an expression for calculating the locations of the inception point for flows over stepped spillways, for longitudinal slope equals 26.6° and  $1 < F^* < 10$ , was obtained.

**Keywords**— Stepped Spillways, Inception Points, Embankments, Overtopping Protection System.

## 1. Introduction

Due to their high-performance with regard to the increase of energy dissipation and decrease of cavitation risks, the stepped spillways have become well-known hydraulic structures widely used in dams engineering [5, 23]. The stepped spillways, due to the steps, can dissipate a significant amount of kinetic energy. Accordingly, a smaller stilling basing is required at the toe of the spillways. In addition, the steps can cause notable aeration which in turn minimizes or eliminates the risks of cavitation. The aeration on stepped spillways is a process at which the air starts to mix vigorously with the flow in which produces an intensively white, fluffy, and bulk flow [5, 14]. The aeration starts where the turbulent boundary layer reaches the free surface of flowing water over a stepped chute is known as the inception point [3, 5, 7, 11, 15, 17].

Inception point locations are typically identified by measuring the distance between the downstream edge of the model crest and the position of occurring of the white fluffy flow [21]. The measurement should be taken parallel to the pseudo-bottom created by the external edges of the steps. Identifying the location of the inception point is essential for the design of stepped spillways stilling basin with regard to cavitation and energy dissipation [12, 13, 19]. Accordingly, the effects

of several step geometries on the inception points of flow over stepped spillways have been explored [1-4, 10, 15, 18, 20-22]. However, the effects of steps with transverse slopes have not been studied so far. The steps with transverse slopes are steps that have slopes perpendicular to the axis of flow in a zigzag pattern; one step has a transverse slope from the right wall towards the left wall while the next step has a transverse slope from the left wall towards the right wall. They are also called non-flat steps. Accordingly, this paper explores the effects of transverse slopes of steps of stepped spillways on the inception points of flows over the stepped spillways. It aims to develop mathematical models and compare them to those developed by the previous researchers.

## 2. Experimental Setup and Procedure

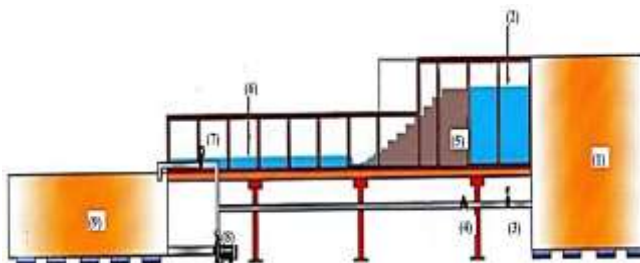
The experiments were carried out at the Hydraulics Laboratory of the College of Engineering at the University of Sulaimani in a prismatic flume. The sides and bottom of the channel were made of Scoret glass having 10 mm thickness. The dimensions of the channel were 0.605 m, 1.35 m, and 8 m for the width, depth, and length respectively. The water was supplied to the channel by a pump having a capacity of 0.05 m<sup>3</sup>/s. Two large tanks, feeding and swamp tanks, were used for circulating the flow. The flow rates during the experiments were measured using an ultrasonic

flowmeter flow; 0.9 to 230 m<sup>3</sup>/h. Figure (1) shows the sketch of the canal, the tanks, the pump, and an installed model.

In this experimental work, three physical models were made from plywood and tested. Each model comprised of a 0.605 m wide broad-crested weir with length  $L_{crest} = 0.6$  m with upstream sharpened corner followed by thirty-two identical steps. The height ( $h$ ) and length ( $h$ ) of the steps were 0.03 m and 0.06 m respectively; the longitudinal slope of the spillway ( $\theta$ ) was 26.6°. Figure (2) and Table (1) provide details on the stepped models used in this experimental study.

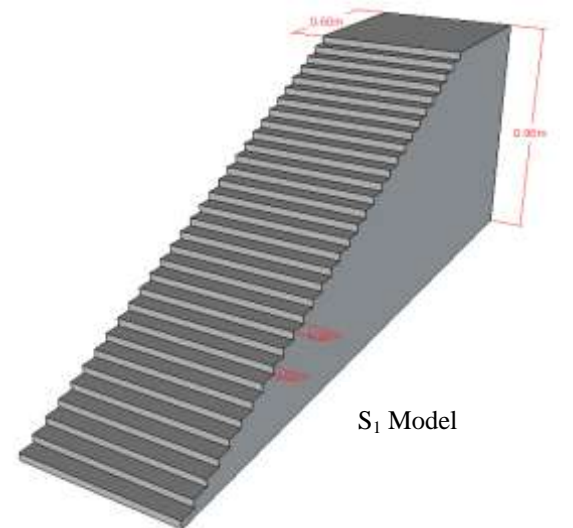
The transverse slope of all steps in the S<sub>1</sub> model was zero; all steps were flat steps. It was considered as the reference model. While in the S<sub>2</sub> and S<sub>3</sub> models, twenty-four steps, after the first step, were non-flat steps. The heights of the steps having transverse slope vary across the flume, see Figure (2) and Table (1). Since there is no transverse slope for the dam crests, the transverse slope of the first step was zero as well. In addition, to prevent non-skewed jumps that may occur downstream of the models, the transverse slope of the last six steps was also zero.

In order to measure water depths along the centerline of the channel during the tests, two point-gauges with 0.1 mm accuracy were used. For each flow rate, the depths of water were measured at two locations; upstream of the models (0.6 m) and downstream of the hydraulic jumps. In addition, the hydraulic jumps were forced to be created just downstream the toe of the spillway using end sills located at the end of the flume.

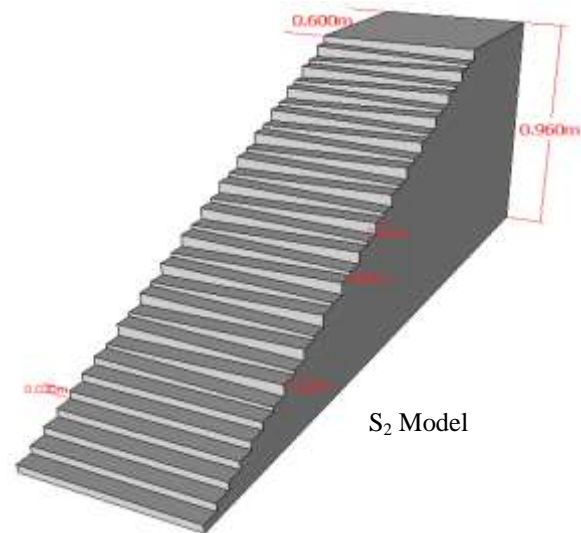


- |                          |                       |
|--------------------------|-----------------------|
| 1. Storage tank          | 6. Point gauge No.2   |
| 2. Point gauge No. (1)   | 7. Bypass valve.      |
| 3. Discharge valve       | 8. Pump.              |
| 4. Ultrasonic flow meter | 9. Recirculation tank |
| 5. Spillway model        |                       |

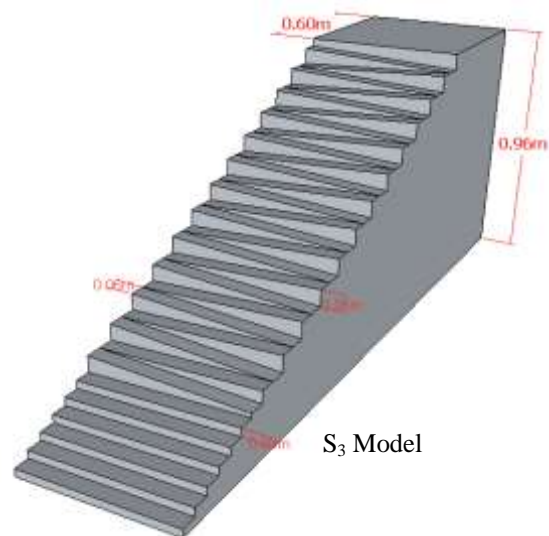
**Figure 1:** Diagram of the experimental setup



S<sub>1</sub> Model



S<sub>2</sub> Model



S<sub>3</sub> Model

**Figure 2:** Sketches for the Physical (S<sub>1</sub>, S<sub>2</sub>, and S<sub>3</sub>) Models

**Table 1:** Description of the Models Investigated in the Study

Models	Step height (m)			Transverse slope, $\alpha$ , degree	$y_c/h$
	At the left side, $h_L$	At the middle, $h_M$	At the right side, $h_R$		
S <sub>1</sub> - 32 flat steps	0.03	0.03	0.03	0	0.56 - 2.78
S <sub>2</sub> - 24 not-flat, 8 flat steps	0.015	0.0225	0.03	1.42	0.55 - 2.78
S <sub>3</sub> - 24 not-flat, 8 flat steps	0.00	0.015	0.03	2.84	0.55 - 2.75

### 3. Result Analysis

For each experiment, the measurements were taken for 7 to 8 hours along visual observations including photographing and videotaping.

#### 3.1 Description of Flow

Visual observations are typically performed in order to identify the flow patterns and regimes for flows over stepped spillways [3, 6, 9, 16]. From the visual observations performed for the current study, the different flow regimes were clearly distinguishable: i.e., nappe, transition, and skimming flow regimes. For small discharges, the nappe flow regimes were observed. The nappe flow regime is identified as a flow regime having a series of free-falling sheets and relatively little aeration [3, 15]. With increasing discharges, a transition flow regime was appeared, which characterized by chaotic behavior and strong splashing and droplet projections downstream of the inception point of free-surface aeration. For larger flow rates, the skimming flow regime prevails. In the skimming flow regime, flow occurs as a consistent stream flowing over an artificial-bottom created by the external edges of the steps. Beneath the pseudo bottom, intense recirculation vortices fill the cavities between all step edges [9, 15]. Table (2) shows the values of  $y_c/h$  corresponding to the flow patterns obtained in this study, where  $y_c$  is the critical depth of flow and  $h$  is step height. The  $y_c$  was calculated using  $y_c = (q_w^2/g)^{1/3}$ , where  $q_w$  is the water unit flow rate and  $g$  is the gravitational acceleration.

**Table 2:** Flow Patterns of the configurations

Models	Flow Patterns		
	Nappe	Transition	Skimming
S <sub>1</sub>	$y_c/h \leq 0.56$	$0.56 < y_c/h < 0.94$	$y_c/h \geq 0.94$
S <sub>2</sub>	$y_c/h \leq 0.98$	$0.98 < y_c/h < 1.47$	$y_c/h \geq 1.47$
S <sub>3</sub>	$y_c/h \leq 1.23$	$1.23 < y_c/h < 2.06$	$y_c/h \geq 2.06$

The results (shown in table (2)) are in good agreement with the previous investigations [6, 15, 16]; they observed the occurrence of the skimming flow at ratio  $y_c/h \geq 0.8$ . From the table, for the S<sub>1</sub> model, the onset of the skimming flow was observed at  $y_c/h \sim 0.94$ . However, for the S<sub>2</sub> and S<sub>3</sub> models, the skimming occurred at larger values of  $y_c/h$ ;  $y_c/h > 2.06$ . This can be attributed to existing non-flat steps in the S<sub>2</sub> and S<sub>3</sub> models. Due to existing non-flat steps in those models, the water over the stepped spillway was moving from one side of the channel to the other side in a zigzag pattern. This, in turn, created cross waves over the stepped spillways along the channel; the free-falling jets crisscrossed each other. Consequently, the characteristics of the skimming flow regimes did not occur except at larger discharges; at larger values of  $y_c/h$ .

#### 3.2 Inception Point Locations

For all three models, in the skimming flows and transition flows to some extent, two contiguous regions of flow over stepped spillways developed; non-aerated and aerated regions. For the non-aerated regions, typically occur over a few upper steps, the surface of the flow is clear and glassy. For the second region, typically occur after the few upper steps, the air starts to mix vigorously with the flow in which produces an intensively white, fluffy, and bulk flow [16, 17, 22]. The latter region starts where the step roughness turbulence, known as a turbulent boundary layer, reaches the free surface.

The locations of the inception point were identified and measured for all three configurations. Figures (3) to (5) show the inception point locations for the three configurations at a similar flow rate.

To evaluate the effects of steps having transverse slopes on the flow properties, the results are plotted as a function of  $y_c/h$  as shown in Figure (6). In the figure, the measured location of the inception points, the lengths of the glassy region ( $L_i$ ), normalized by  $k_s$ , where  $k_s = h \cdot \cos \theta$ . The relationships were constructed for skimming flows,  $y_c/h > 1$ .

From Figure (6), for similar  $y_c/h$  ratios, the lengths of the glassy region for the flows over the S<sub>1</sub> model,  $L_i$ , were greater than those for the S<sub>2</sub> and S<sub>3</sub> models. For similar

$y_c/h$  ratios, the lengths of the glassy region for the flows over the  $S_2$  model decreased to 75%, on average, compared to the lengths of the glassy region for flows over the  $S_1$  model. Regarding the  $S_3$  model, the values of  $L_i$  decreased to 63%, on average. The reduction can be due to the existence of the non-flat steps. Because of the existing non-flat steps, the flow velocity was not uniformly distributed across the flume. This, in turn, led to creating cross waves. In addition, walls slightly raised the water surfaces. This, as well, created some small waves which finally fallen into the main streamflow. Consequently, extensive turbulent flows closer to the downstream edge of the spillway crest were formed which, in turn, reduced the lengths of the glassy region for the flows; reducing the values of  $L_i$ .



Figure 3: Inception point location for  $S_1$  model with discharge of  $0.0323 \text{ m}^3/\text{s}$

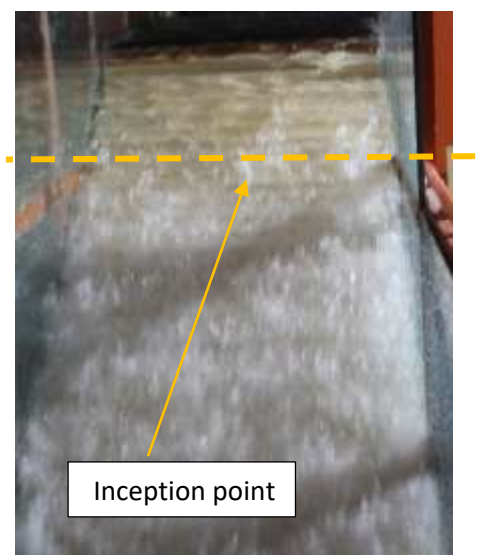


Figure 4: Inception point location for  $S_2$  model with discharge of  $0.0311 \text{ m}^3/\text{s}$

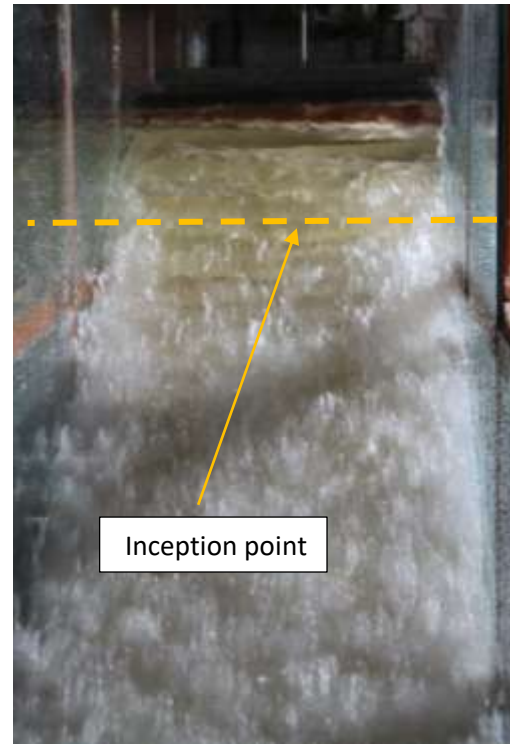


Figure 5: Inception point location for  $S_3$  model with discharge of  $0.0319 \text{ m}^3/\text{s}$

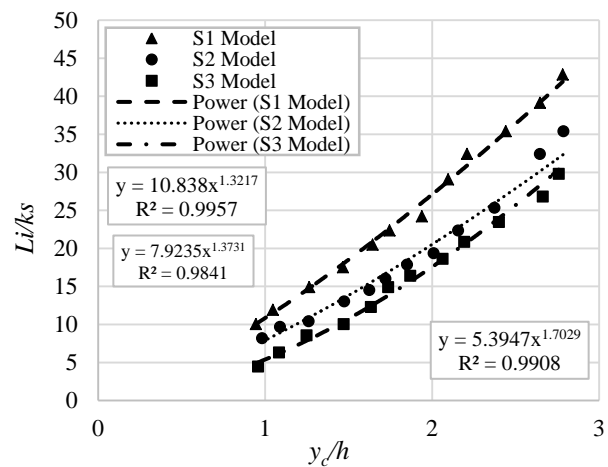


Figure 6: Dimensionless location of the inception point ( $L_i/k_s$ ) versus dimensionless discharge  $y_c/h$  – for ( $S_1$ ,  $S_2$ , and  $S_3$ ) models.

Hunt and Kadavy (2011) [21] developed an expression for the inception point locations taking into account roughness Froude number,  $F^*$ , as shown below:

$$L_i = 5.38 * F^{*0.86} * k_s \quad (1)$$

where  $F^* = \{q_w / [g * (\sin \theta) * (k_s)^3]^{1/2}\}$ .

For the comparison purpose, Figures (7) to (10) were constructed in order to evaluate the measured  $L_i$  normalized by  $k_s$  against  $F^*$ , From the figures, the

relationships followed the power trend and can be represented best by the following equations:

$$L_i = 6.5606 * F^{*0.8812} * k_s \quad (2)$$

$$L_i = 4.7035 * F^{*0.9154} * k_s \quad (3)$$

$$L_i = 2.8254 * F^{*1.1353} * k_s \quad (4)$$

$$L_i = 4.4232 * F^{*0.979} * k_s \quad (5)$$

with the coefficients of determination,  $R^2$ , very close to 1.0 except for Figure (10);  $R^2 = 0.8398$ .

From Eqs. (1) and (2), the results of this study are promising. However, the differences between Eqs. (1) and (2) can be attributed to using different  $\theta$ . Hunt and Kadavy (2011) in [21] used  $\theta = 22$ , while the  $\theta$  used in this study is  $26.6^\circ$ . In addition, since the point of inception on stepped spillway is identified by visual observation, the results can be slightly different from one researcher to another [3]. The differences between Eqs. (2) - (4) are assumed to be a result of existing non-flat steps.

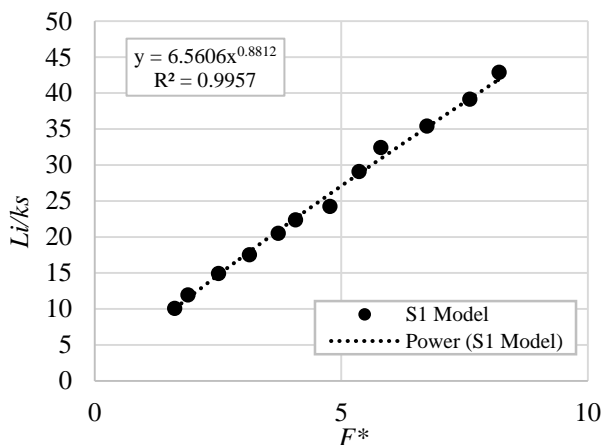


Figure 7:  $L_i/k_s$  versus  $F^*$  - S<sub>1</sub> model

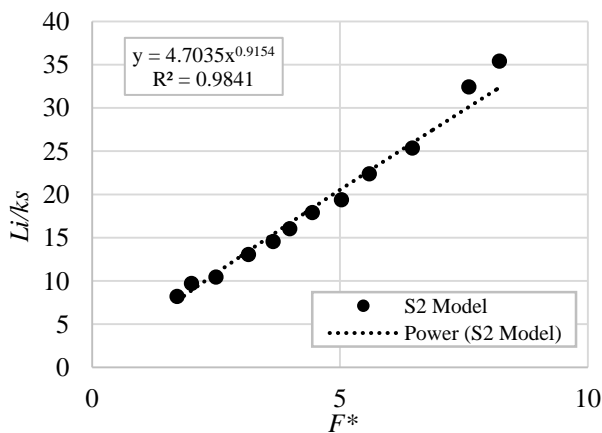


Figure 8:  $L_i/k_s$  versus  $F^*$  - S<sub>2</sub> model

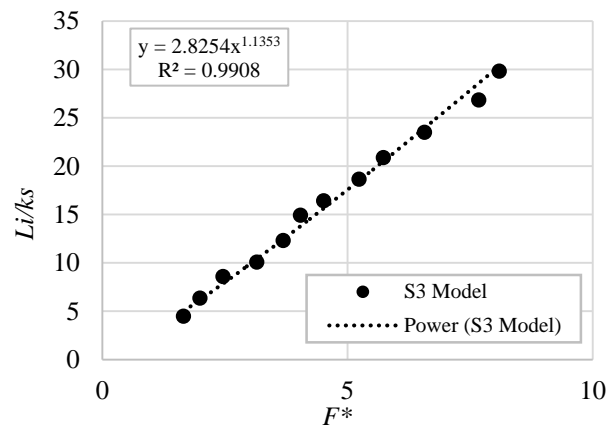


Figure 9:  $L_i/k_s$  versus  $F^*$  - S<sub>3</sub> model

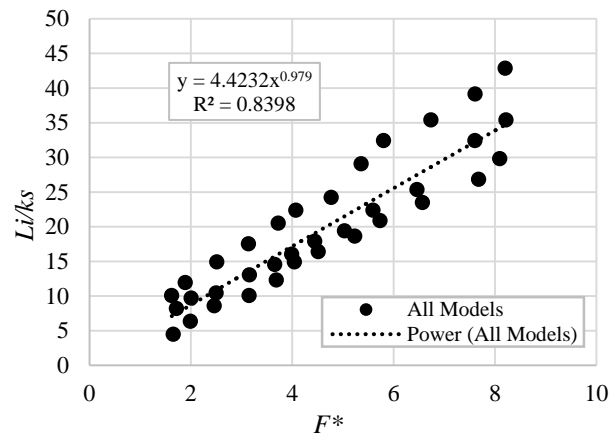
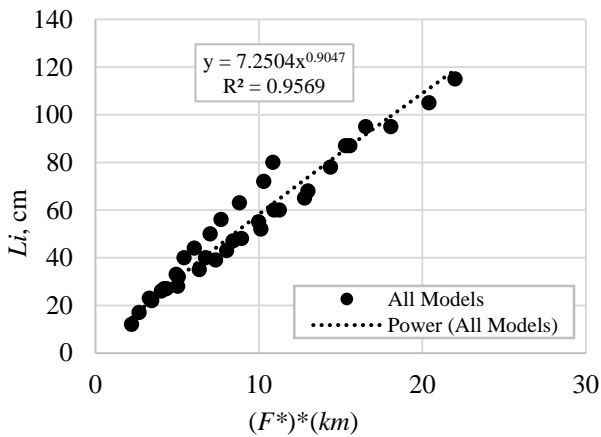


Figure 10:  $L_i/k_s$  versus  $F^*$  - All Models

Although the data in Figure (10) gave a good correlation, they showed a slight scattering compared to the other correlations. Accordingly, the results were further analyzed seeking more accurate expression for predicting  $L_i$ . For this purpose, Figure (11) constructed to evaluate the measured  $L_i$  divided by modified  $k_m$ , where  $k_m = [h_M * \cos \theta]$ ; the height of the steps in the middle of the channel,  $h_M$  were used instead of the normal height of the steps,  $h$ . The relationships followed the power trend and can be represented best by the following equations:

$$L_i = 7.2504 * F^{*0.9047} * k_m \quad (6)$$

with the coefficients of determination,  $R^2$ , close to 1.0. The results gave a decent correlation for  $\theta = 26.56^\circ$  and  $1 < F^* < 10$ . This means that the modification could improve the correlation by increasing the value of  $R^2$  from 0.8394 to 0.9569.



**Figure 11:** Location  $L_i/k_s$  versus  $(F^*) \cdot km$ - All Models

#### 4. Conclusions

An experimental study was performed to explore the effects of non-flat steps on the inception point positions for flows over the stepped spillways. Three wooden models with  $(\theta = 26.6^\circ$  or 1V:2H) were constructed and tested. From the visual observations, different flow patterns were observed. However, for the stepped spillways containing non-flat steps, the onset of the skimming flow occurred at higher discharges; at the ratios of critical depth ( $y_c$ ) to step height ( $h$ ) greater than or equal to 2.06. In addition, the results showed that the values of  $L_i$ , the distance of the inception points from the spillway crest, decreased due to the existence of the non-flat steps; for the model containing non-flat steps ( $\alpha = 2.84^\circ$ ) the value of  $L_i$  decreased by 37%. Furthermore, an improved correlation for obtaining the values of  $L_i$  is provided for  $\theta = 26.6^\circ$  and  $1 \leq F \leq 10$ . Additional researches are recommended for different longitudinal and transverse slopes to further validate these findings.

#### Acknowledgments

The experiments were carried out using the facility at the College of Engineering, University of Sulaimani.

#### References

- [1] ASCE Task Committee, "Alternatives for overtopping protection of dams," ASCE, New York, 139p, 1994.
- [2] C. A. Gonzalez, and H. Chanson, "Air entrainment and energy dissipation on embankment spillways," International Symposium on Hydraulic Structures, Ciudad Guayana, Venezuela, 2006.
- [3] H. Chanson "Stepped spillway flows and air entrainment," Canadian Journal of Civil Engineering, vol. 20, no. 3, pp. 422-435, 1993.

- [4] H. Chanson, "Embankment overtopping protection systems," Acta Geotechnica, vol. 10, no. 3, pp.305-318, 2015.
- [5] H. Chanson, "Hydraulic Design of Stepped Cascades, Channels," Weirs and Spillways, Pergamon, Oxford, UK, 1994.
- [6] H. Chanson, "Hydraulic design of stepped spillways and downstream energy dissipators," Dam Engineering, vol. 11, no. 4, pp. 205-242, 2001.
- [7] H. Chanson, "The hydraulics of stepped chutes and spillways," A. A. Balkema Publishers, Lisse, 2002.
- [8] H. Chanson, and S. Felder, S., "Energy dissipation on embankment dam stepped spillways, overflow stepped weirs and masonry stepped spillways," In Proceedings of the 17th Congress of IAHR Asia and Pacific Division, Auckland, New Zealand (Melville B, Costa GD and Swann T (eds)). 2010.
- [9] I. Ohtsu, Y. Yasuda, and M. Takahashi, "Flow characteristics of skimming flows in stepped channels," Journal of Hydraulic Engineering, ASCE, vol. 130, no. 9, pp 860-869, 2004.
- [10] K. H. Frizell, "Protecting embankment dams with concrete stepped overlays," Hydro Review, vol. 16, no. 5, 1997.
- [11] M. Bindo, J. Gautier, and F. Lacroix, "Stepped spillway of M'Bali dam." International water power and dam construction, vol. 45, no. 1, pp. 35-36, 1993.
- [12] M. Pfister, and W. H. Hager, "Self-entrainment of air on stepped spillways," International Journal of Multiphase Flow, vol. 37, no. 2, pp. 99-107, 2011.
- [13] M. Pfister, W. H. Hager, H. E. Minor, "Stepped chutes: Pre-aeration and spray reduction," International Journal of Multiphase Flow, vol. 32, no. 2, pp. 269-284, 2006.
- [14] M. R. Chamani, "Air inception in skimming flow regime over stepped spillways," Proceedings, International Workshop on Hydraulics of Stepped Spillways, Balkema, Rotterdam, The Netherlands, pp. 61-67, 2000.
- [15] M. R. Chamani, and N. Rajaratnam, "Onset of skimming flow on stepped spillways," Journal of Hydraulic Engineering, ASCE, vol. 125, no. 9, pp. 969-971, 1999.
- [16] N. Rajaratnam, "Skimming flow in stepped spillways," Journal of Hydraulic Engineering, ASCE, vol. 116, no. 4, pp 587-591, 1990.
- [17] R. Wood, P. Ackers, and J. Loveless, "General method for critical point on spillways," Journal of Hydraulic Engineering, ASCE, vol. 109, no. 2, pp. 308-312, 1983.
- [18] S. Felder, "Air-water flow properties on stepped spillways for embankment dams: Aeration, energy dissipation and turbulence on uniform, non-uniform and pooled stepped chutes" Doctoral Thesis, The University of Queensland, 2013.

- [19] S. L. Hunt, and K. C. Kadavy, "Energy dissipation on flat-sloped stepped spillways: Part 1. Upstream of the inception point," Transactions of the ASCE, vol. 53, no. 1, pp. 103-109, 2010.
- [20] S. L. Hunt, and K. C. Kadavy, "Energy dissipation on flat-sloped stepped spillways: Part 2. Downstream of the inception point," Transactions of the ASABE, vol. 53, no. 1, pp. 111-118, 2010.
- [21] S. L. Hunt, and K. C. Kadavy, "Inception point relationship for flat-sloped stepped spillways," Journal of Hydraulic Engineering, ASCE, vol. 137, no. 2, pp. 262-266, 2011.
- [22] T. Hepler, B. Crookston, and J. Crowder, "Successful overtopping protection projects in the Eastern US," 2018.
- [23] W. Wan, R. Awais, and X. Chen. "Effect of Height and Geometry of Stepped Spillway on Inception Point Location." Applied Sciences, vol. 9, no. 10, pp. 1-14, 2019.

## آثار المنحدرات المستعرضة للخطوات على مواقع نقطة الانطلاق من التدفق على المسيلات المتدرجة

ناهنگ صلاح علي<sup>1</sup>، اميد سعيد قادر يوسف<sup>2\*</sup>

<sup>1</sup> جامعة السليمانية، السليمانية، العراق، ahang.ali@univsul.edu.iq

<sup>2</sup> جامعة السليمانية، السليمانية، العراق، omed.qadir@univsul.edu.iq

\* الباحث الممثل: اميد سعيد قادر يوسف، omed.qadir@univsul.edu.iq

نشر في: 30 ايلول 2020

**الخلاصة** – في هذه الدراسة التجريبية، تم اختبار تأثير الميل العرضي لمدرجات المسيل المائي على موقع نقطة بداية الجريان المضطرب (Inception point location). المدرجات ذات الميل العرضي هي التي لها ميول من الجدار الايمن للمسيل باتجاه الجدار الايسر للمسيل وبالعكس في نمط مترادف (zigzag). لغرض اجراء الدراسة تم اعداد ثلاثة نماذج خشبية للمسيل المدرج في قناة مختبرية منتظمة (prismatic flume). ابعاد المسيل المدرج ذات الاثنتين وثلاثين تدرجاً كانت بعرض و عمق و طول 0.6م، 0.96م و 1.92م على التوالي. تم قطع اثنان و ثلاثون تدرجاً (مع ثلاثة الميالات العرضية المختلفة من صفر الى  $2.84^{\circ}$ ) من (crest) الى (toe). اظهرت النتائج أن بعد نقاط بداية الجريان المضطرب (Inception point) عن الحافة الدنيا (Downstream edge) للهدارة ذات السطح العريض قد قلت بمعدل 37% بالنسبة للمسيل المدرج ذات الميل العرضي  $2.84^{\circ}$ . ان نقطة بدء الجريان الانزلاقي (skimming flow) للنماذج المدرجة ذات الميول العرضية تحدث عند نسب عمق حرج (yc) الى ارتفاع التدرج (h) أكبر او يساوي 2.06. اضافةً الى ذلك تم تطوير معادلة رياضية للتنبؤ بموقع نقطة بدء الجريان المضطرب قابل للتطبيق على المسيلات المدرجة ذات الميل (26.5 درجة) و ذات رقم فراود ( $1 < F^* < 10$ ).

**الكلمات الرئيسية** – المسيل المائي المدرج، نقطة البدء، السدود الركامية، نظام الحماية ضد طفح المياه.